

# Radar Cross Section Dependence on Wind Speed

David G. Long, Ben E. Barrowes, David V. Arnold  
Microwave Earth Remote Sensing (MERS) Laboratory  
Brigham Young University, Electrical and Computer Engineering Dept.  
459 Clyde Building, Provo, UT 84602  
801-378-4383, FAX: 801-378-6586, e-mail: long@ee.byu.edu

*Abstract*—YSCAT was an ultrawideband (2–20 GHz), near constant beamwidth scatterometer intended to provide radar cross section measurements at varying radar and environmental parameters. YSCAT was deployed on the CCIW (Canada Center for Inland Waters) tower on Lake Ontario for a period of six months in 1994. Using YSCAT data, this paper reports 1) observance of a “low wind-speed cutoff”, the fall-off of  $\sigma_0$  which occurs at low wind speeds, and 2) the results of a fitting 2-component lognormal/Rayleigh combined probability distribution to the observed backscattered power measurements at C-band (5 GHz) and X-band (10 GHz). The observed characteristic trends of the fitted pdf model parameters versus wind speed are shown and discussed.

## INTRODUCTION

YSCAT was developed to study the air-sea interface under varying radar and environmental parameters [4]. In one of its operational modes YSCAT collected data at five principal frequencies of 2, 3.05, 5.3, 10.02, and 14 GHz, eight incidence angles of 0 (nadir), 10, 20, 25, 30, 40, 50, and 60°, and at both horizontal and vertical polarizations. In this mode the azimuth angle of YSCAT was adjusted to track the wind direction, with both up wind and down wind measurements obtained. Sorting the recorded data according to wind speed, 1600 distinct cases of the previous parameters emerge on which to draw conclusions which may increase understanding of the air-sea interface.

Analysis of each of the 1600 cases separately would be impractical in this setting; instead, an analysis of a few cases at wind speeds of 1–10 m/s is presented. Results will be summarized and compared to other cases and the implications discussed.

## LOW WIND SPEED CUTOFF

Donelan and Pierson [5] postulated the existence of a low wind roll off in  $\sigma_0$  versus wind speed. At very low wind speeds, the friction velocity is too small to generate small waves, resulting in a smooth surface and a small backscatter cross section. At higher wind speeds, the wind generates capillary waves and  $\sigma_0$  closely follows a power-law relationship with wind speed. This effect has been observed in carefully controlled wave tank data where a hysteresis effect in  $\sigma_0$  versus wind speed is observed [6]: as the wind speed is increased from zero, at a temperature-dependent threshold wave generation commences and  $\sigma_0$  in-

creases significantly. As the wind speed is decreased, waves are maintained at wind speeds below the startup threshold and finally fall off. The thresholds at which wave generation begins and ends is very temperature and long wave field sensitive.

While this effect has been observed in wave tank data [6] and in airship scatterometer data [7], it has not previously been reported in tower data. However, YSCAT data provides strong evidence to support this low wind speed roll off over a wide range of frequencies. For example, Fig. 1 illustrates a typical plot of YSCAT  $\sigma_0$  versus wind speed. This example is for 3 GHz at 20° incidence and is typical of YSCAT data. We note that there is a dramatic falloff in the received power at wind speeds less than about 4 m/s. The broad wind speed spread in the falloff region supports the hysteresis effect observed in wave tank data since there is a range of long wave and temperature conditions as well as wind fluctuations in the uncontrolled environment of the tower experiment. We postulate that the fall off has not been observed in space borne scatterometer measurements due to wind variability over the large area footprints of such instruments. Over the range of frequencies and incidence angles observed by YSCAT, the fall off threshold varies from 3 to 6 m/s.

## 2-COMPONENT LOGNORMAL/RAYLEIGH DISTRIBUTION

Thompson and Gotwols [1] proposed a probability distribution for modeling microwave radar backscatter based on conditional

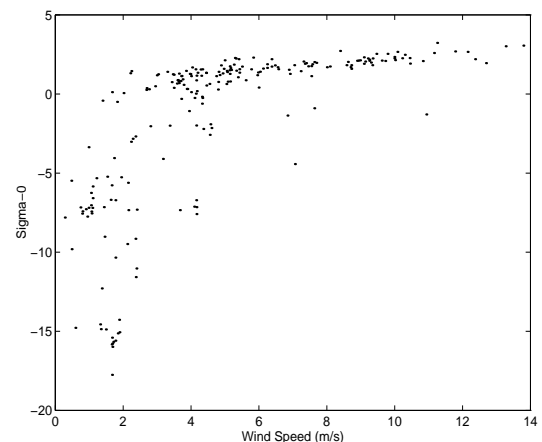


**Figure 1:** Typical YSCAT backscatter response illustrating the low wind speed roll off of  $\sigma_0$ . Data is for 3 GHz, vertical polarization, upwind, 20° incidence angle.

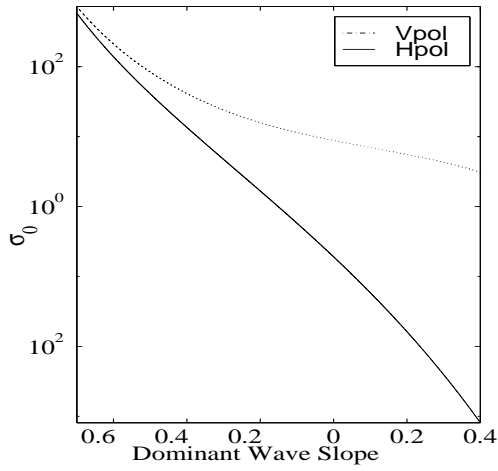


**Figure 2:** Dominant wave slope versus  $\sigma_o$  plotted from the Donelan spectrum [2]. 14GHz, wind speed 8m/s, fetch is 9km.

probabilities,

$$p(a) = \int_0^{\infty} p(a|\sigma_o)p(\sigma_o)d\sigma_o. \quad (1)$$

This model for radar backscatter from water waves assumes that the wave spectrum consists of two scales of waves: waves smaller than the dominant wave length but on the order of the scatterometer footprint or smaller, and dominant wavelength waves larger than the scatterometer footprint. On scales shorter than the longer dominant waves,  $\sigma_o$  is assumed to be constant with amplitude becoming a conditional probability  $p(a|\sigma_o)$ . For longer wavelengths,  $\sigma_o$  varies yielding the probability  $p(\sigma_o)$ .

The distribution of  $p(a|\sigma_o)$  has been debated, with Thompson and Gotwols [1] concluding that for their data,  $p(a|\sigma_o)$  was Rayleigh distributed. YSCAT's backscatter sampling frequency of 10 Hz is too low to test its data by removing the underlying  $p(\sigma_o)$  dependence as does [1]. The present analysis assumes that  $p(a|\sigma_o)$  is indeed Rayleigh distributed.

The distribution of  $p(\sigma_o)$  can be derived by starting at the theoretical result for  $\sigma_o$  given by small perturbation theory [1]

$$\sigma_o = 16\pi k_m^4 |g_{ii}(\theta_i)|^2 \Psi(2k_m \sin \theta_i, 0). \quad (2)$$

The wave height spectral density ( $\Psi$ ) is assumed to be a Donelan spectrum since it was developed by Donelan using wave staff data taken at the same site where YSCAT was deployed. Using the definitions given in [2], and writing  $p(\sigma_o)$  in terms of  $p(s_x)$  using the transformation law

$$p(a) = \frac{p(s_x)}{|d\sigma_o/ds_x|} \quad (3)$$

where  $s_x$  is the dominant wave slope, yields the relationship between  $s_x$  and  $\sigma_o$  illustrated in Fig. 2. The shape of these curves for mid-range incidence angles can be reasonably approximated by a first or second order fit in log space [1]. Thus, in general,  $\sigma_o$  may be expressed as a two component exponential

$$\sigma_{op} = C e^{a_1 s_x + a_2 s_x^2} \quad (4)$$

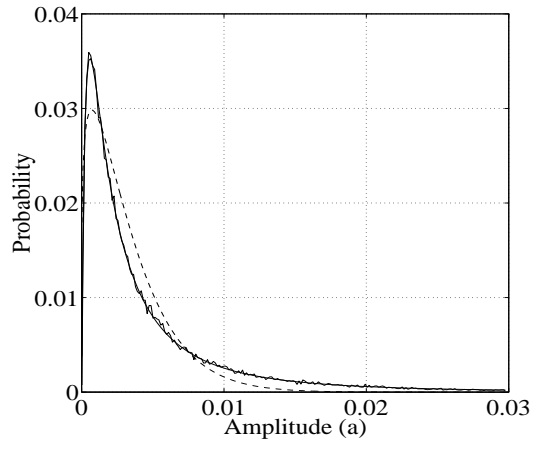


**Figure 3:** Weibull and Rayleigh/Lognormal Distributions fitted to YSCAT data. Weibull distribution shown as dashed line. The Rayleigh/lognormal distribution is obscured by the data due to the excellent fit. Data is 5 GHz, v-pol, downwind, 20°, 2 m/s. Rayleigh/lognormal parameters are  $a_1=17.57$ ,  $a_2=-5.58$ ,  $\sigma_x=0.0914$ , and  $C=5.85e4$ .

where  $p$  is either  $v$  or  $h$ , and  $p(\sigma_o)$  may be expressed using Eq. 3 as [1]:

$$p(\sigma_{oh}) = \frac{1}{a_1 \sigma_x \sigma_{oh} \sqrt{2\pi}} \exp \left\{ \frac{-(\ln \sigma_{oh} - \ln C)^2}{2a_1^2 \sigma_x^2} \right\} \quad (5)$$

for horizontal polarization, and

$$p(\sigma_{ov}) = \frac{1}{(a_1 + 2a_2 s_x) \sigma_x \sigma_{ov} \sqrt{2\pi}} \exp \left\{ \frac{-(s_x)^2}{2\sigma_x^2} \right\} \quad (6)$$

for vertical polarization, with  $s_x$  defined by Eq. 4 assuming  $p(s_x)$  is normally distributed.

### FITTING THE DISTRIBUTION

Knowing functional forms for both  $p(a|\sigma_o)$  and  $p(\sigma_o)$ , and again using Eq. 3, Eq. 1 may be written as:

$$p(a) = \int_{-\infty}^{\infty} \underbrace{2aC e^{a_1 s_x + a_2 s_x^2} e^{-a^2 C e^{a_1 s_x + a_2 s_x^2}}}_{p(a|\sigma_o(s_x))} \underbrace{\frac{e^{-\frac{s_x^2}{2\sigma_x^2}}}{\sqrt{2\pi}\sigma_x}}_{p(\sigma_o(s_x))} ds_x. \quad (7)$$

The analytical solution to this integral has not been found by the authors. However, this integral may successfully be evaluated numerically. For any given values of  $a_1$ ,  $a_2$ ,  $\sigma_x$ , and  $C$ , this integral can be numerically approximated for any value of  $a$ . When tabulated for a sufficient number of  $a$ 's, a distribution emerges. This distribution can then be fit to actual data. An example is given in Fig. 3.

In the majority of cases, the Rayleigh/lognormal combined distribution fits YSCAT data extremely well. Distributions were fit to YSCAT data by minimizing the Kullback-Leibler distance [3], which provides a measure of the "distance" between two

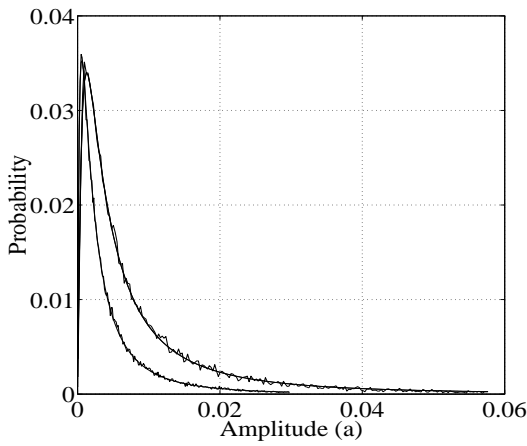


**Figure 4:** Backscatter distributions for 5 GHz, v-pol, downwind, 20°, 2 and 6 m/s. Lower curve is for 2 m/s. Parameters for 6 m/s case are  $a_1=19.2$ ,  $a_2=-14.8$ ,  $\sigma_x=0.0914$ , and  $C=2.14e4$ .

distributions and is given by

$$p(f||g) = \int f(x) \log \frac{f(x)}{g(x)} dx. \quad (8)$$

All of the YSCAT data has been parameterized with this distribution. Care must be taken because in four variables,  $a_1$ ,  $a_2$ ,  $\sigma_x$ , and  $C$ , Eq. 7 is degenerate (*i.e.* it has non-unique solutions). However,  $\sigma_x$  may be calculated from *in situ* wave staff measurements. Choosing  $\sigma_x$  guarantees a unique solution. For simplicity, all cases presented in this paper use  $\sigma_x = 0.0914$ . One example of the fitted distribution is shown in Fig. 3, another in Fig. 4 with the previous distribution included for reference.

The two distributions are significantly different with the 6 m/s case having a much longer tail and greater mean. This difference is reflected in the fitted parameters with increasing

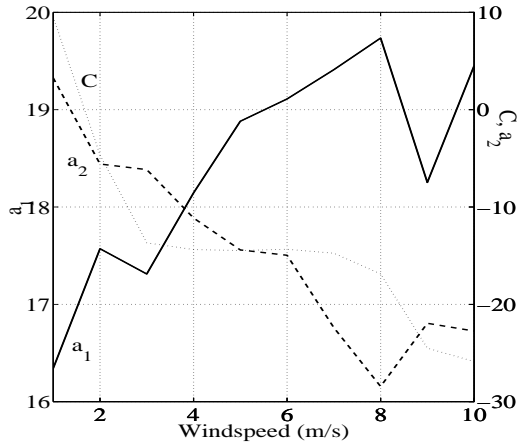


**Figure 5:**  $a_1$ ,  $a_2$ , and  $C$  values for 5 GHz, v-pol, downwind, 20°, 1-10 m/s.  $C$  values are scaled by the relation  $20 \log_{10}(C) - 100$ .

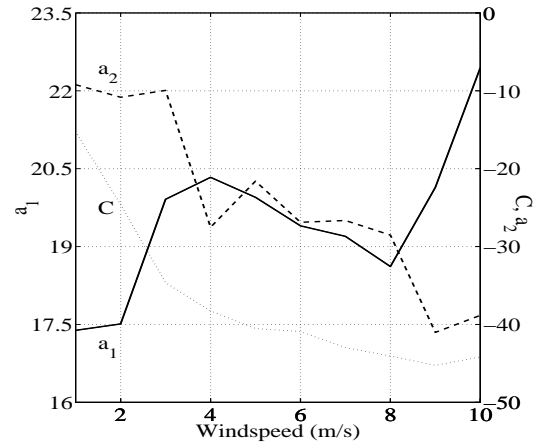


**Figure 6:**  $a_1$ ,  $a_2$ , and  $C$  values for 10 GHz, v-pol, downwind, 20°, 1-10 m/s.  $C$  values are scaled by the relation  $10 \log_{10}(C) - 100$ .

$a_1$  and decreasing  $a_2$  and  $C$ . This is a common trend in YSCAT data. Figures 5 and 6 show parameter values for data at 5 and 10 GHz respectively.

## DISCUSSION

Backscatter distributions from YSCAT at 5 and 10 GHz, v-pol, downwind, 20°, 1-10 m/s were shown to exhibit characteristic trends when parameterized by a combined Rayleigh/lognormal distribution. These trends could prove useful in increasing our understanding of the effect of environmental parameters on radar backscatter.

## REFERENCES

- [1] Gotwols, B. L., and D.R. Thompson, "Ocean Microwave Backscatter Distributions" *Journal of Geophysical Research*, vol. 99, no. C5, pp. 9741-9750, May 15 1994.
- [2] Donelan M. A., J. Hamilton, and W. H. Hui, "Directional Spectra of Wind-Generated Waves" *Philosophical Transactions of the Royal Society of London*, vol. 315, no. A, pp. 509-562, 1985.
- [3] Cover T. M., and J. A. Thomas, "Elements of Information Theory", New York: Wiley, 1990.
- [4] Long D. G., R.S. Collyer, R. Reed, and D.V. Arnold, "Dependence of the Normalized Radar Cross Section of Water Waves on Bragg Wavelength-Wind Speed Sensitivity," *IEEE Transactions on Geoscience and Remote Sensing*, Vol. 34, No. 3, pp. 656-666, May 1996.
- [5] Donelan, M. A., and W.J. Pierson, Jr., "Radar Scattering and Equilibrium Ranges in Wind-Generated Waves with Application to Scatterometry," *J. Geophys. Res.*, Vol. 92, pp. 4971-5029, 1987.
- [6] Plant W. J., W.C. Keller, M.A. Donelan, and D.E. Weissman, "A Wind Speed Threshold in Microwave Scattering from the Ocean", URSI Meeting, Boulder, CO, 1999.
- [7] Plant, W.J., D.E. Weissman, W.C. Keller, V. Hesany, K. Hayes, and K.W. Hoppel, "Air/sea momentum transfer and the microwave cross section of the sea", in press *J. Geophys. Res.*